buildings

MDPI

Article

A Study of Preload Detection Technology in Suspension Bridge Cable Clamp Bolts Based on the Pull-Out Method

Fengrui Mu [1], Gui Zhu [2], Yongjun Zhou [1,*], Zhongguo John Ma [3], Yuan Jing [1] and Yu Zhao [1]

1 School of Highway, Chang'an University, Xi'an 710064, China; 2022121078@chd.edu.cn (F.M.)
2 Guangxi Xingang Transportation Investment Co., Ltd., Qinzhou 535000, China
3 Department of Civil and Environmental Engineering, University of Tennessee, Knoxville, TN 37996, USA
* Correspondence: zyj@chd.edu.cn

Abstract: The pull-out method is a simple and effective method for detecting the preload of suspension bridge cable clamp bolts. However, research on the pull-out method is currently limited. The force principles governing the bolt during the pulling process are unclear, and the relationship between tension force and the desired preload remains uncertain. This paper aims to explore the force principles of bolts during the pull-out method detection process through a combined approach of theoretical analysis, full-scale test, and finite element simulation. The results indicate that the bolt preload increases during the pulling process. The preload detected by the pull-out method is not the initial preload of the bolt, but rather it exceeds the initial preload. The force relationships among various components are determined as follows: the preload subtracts the change value of the force exerted by the nut at the tension end, which equals the change value of tension force. Additionally, an analysis of the impact of the length of the bolt clamping section and the bolt area on the preload was conducted. Under the same bolt area, a shorter clamping section length corresponds to a greater increase in preload. With the same clamping section length, the increment of preload increases with the bolt area. These findings can serve as references for detecting and specifying the preload of the bolts.

Keywords: civil engineering; suspension bridge; pull-out method; cable clamp; preload detection

Citation: Mu, F.; Zhu, G.; Zhou, Y.; Ma, Z.J.; Jing, Y.; Zhao, Y. A Study of Preload Detection Technology in Suspension Bridge Cable Clamp Bolts Based on the Pull-Out Method. *Buildings* **2024**, *14*, 976. https://doi.org/10.3390/buildings14040976

Academic Editor: Fabrizio Gara

Received: 8 March 2024
Revised: 26 March 2024
Accepted: 28 March 2024
Published: 2 April 2024

1. Introduction

The cable clamp on a suspension bridge acts as the critical connection and force transfer component between the main cable and the suspender, facilitating the transfer of tension. However, due to various factors, the high-tensile bolts are subjected to force degradation [1]. When the applied force on these bolts drops to a certain level, it can cause the loosening or slipping of the cable clamps, leading to modifications within the cable and a redistribution of internal forces throughout the suspension bridge [2]. Consequently, this poses a substantial risk to the structural safety of suspension bridges. Bridge detection data are of crucial use in evaluating bridge safety [3–5]. Therefore, it is essential to check the tightness of the bolted cable clamp regularly.

Common detection methods include the torque wrench, ultrasonic, sensor, and pull-out methods. Current research in bolt detection technology focuses primarily on small bolt components in the mechanical field and wind power generation projects. The torque wrench method relies on understanding the distribution ratio of bolt torque and its relationship to preload. In torque distribution, only 10–15% of the torque is used to rotate the bolt, and the remaining 85–90% is reserved for overcoming the prevailing friction [6]. Estimating bolt preload using the torque wrench method is susceptible to external factors, such as the coefficient of friction, thread tolerance errors, and the type of lubricant coating [7–9]. As a result, this method is prone to yielding measurements with an error of more than 20% in bolt preload measurements [10]. Despite the torque wrench method being systematically used in wind energy projects, it is difficult to obtain the K-factor accurately. Its lower accuracy and reliability make the detected bolt preload unreliable. First, in suspension bridges, the bolts and nuts are susceptible to corrosion, making the error of the torque wrench method more likely to be magnified. Second, to save labor, it is necessary to increase the strength arm, which introduces operational inconveniences. Third, the risk of aerial operations on the suspension bridge also increases.

The ultrasonic method establishes a correlation between ultrasonic wave velocity or acoustic time differences and bolt preload. It estimates the preload by measuring ultrasonic physical parameters associated with the bolts [11–14]. To improve the accuracy of ultrasonic measurements and to reduce the influence of environmental factors during the measurement process, Kim et al. [15] introduced a novel mode conversion ultrasonic technology. Chen et al. [16] proposed a time-frequency parameter identification method based on the Gabor transform and a novel axial stress evaluation model for bolts. To minimize the influence of ambient temperature, Pan et al. [17] established a mathematical model for measuring bolt preload during assembly, taking into account the shape factor and combining both longitudinal and transverse waves. Though the ultrasonic method is portable and convenient to operate, in-the-air pre-calibration is necessary and several factors contribute to errors in ultrasonic measurements, such as temperature, the thickness of the coupling agent [18], and the position of the ultrasonic probe [19]. Furthermore, the presence of slight defects in the bolt can cause waveform disturbances that lead to the inaccurate determination of preload.

In the field of using sensors to determine the preload of the bolts, Nazarko et al. [10,20] used piezoelectric transducers to develop a non-destructive testing method for determining the preload of the bolts. Herbst et al. [21] innovatively designed a force-measuring bolt by integrating a force sensor directly into the bolt structure, allowing real-time monitoring of the bolt's stress state. Tu et al. [22] pioneered the use of metal-encapsulated Fiber Bragg Grating (FBG) sensors to measure bolt preload. Wang et al. [23] developed a strain sensor to measure axial force by exploiting the linear relationship between the radial strain on the top surface of the bolt and the applied preload. Liu et al. [24] implemented high-frequency piezoelectric film sensors on bolts and developed a non-destructive bolt preload measurement system. In another approach, Jiménez-Peña et al. [25] used computer vision sensors to measure bolt elongation as a means of estimating bolt preload. In addition, Gotoh et al. [26], Mori et al. [27], and Hasebe et al. [28] measured bolt preload by monitoring changes in magnetic flux density. The sensor-based approach allows real-time monitoring of bolt preload but is associated with high deployment and measurement costs. In addition, the narrow space on suspension bridge platforms poses challenges for installing, maintaining, and replacing certain sensor types on cable clamp bolts. Additionally, some of these sensors have limited measurement capabilities, which are unsuitable for determining the preload of high-strength bolts used in cable clamps.

The pull-out method typically involves mechanically pulling the bolt using a hydraulic jack. When the load applied by the hydraulic jack equals the axial force of the bolt, the nut will unload and loosen. At this point, the load applied by the hydraulic jack is considered to be the desired preload. In general, the characteristics of preload detection for bolts used in suspension bridge cable clamps include high-preload, high-altitude operations, and limited testing platforms. Compared to other methods, the pull-out method is more straightforward, less affected by environmental factors, and better suited for suspension bridges. Currently, there is limited research on the pull-out method; Hashimura et al. [29,30] contended that the pull-out method can precisely control the preload, and obtained the relationship between the change in the stress-free portion's elongation at the bolt's end during the pulling process. Hashimura et al. [31] proposed to use the pull-out method to detect the stiffness of the bolt clamping section, but the detected stiffness had a large error compared with the theoretical value. In the study of errors in the pull-out method, Hashimura et al. [32,33] discussed the sources of errors in the pull-out method of detection and considered that the verticality of the bearing surface and the thread gap were the main factors causing errors, and found that the pull-out method is highly robust with regard to the verticality error of the bolt-bearing surface.

These studies generally consider that the point corresponding to the sudden change in elongation corresponds to the tension force, which is the bolt's preload. Similarly, they only investigated the control and detected effect of the pull-out method on preload. However, for large high-preload bolts, the force principles acting on the bolt during the pulling process are not clear, and the relationship between tension force and desired preload is uncertain. Based on the bolt preload pull-out method detection technology, this paper elucidates the force principles involved in the pull-out detection process and investigates the influence of bolt physical parameters on the bolt force. Initially, a theoretical analysis is conducted to derive the theoretical formula for the variation of bolt preload during the pull-out detection process, along with theoretical equations describing the force relationships among various components. Subsequently, full-scale tests are performed to validate the correctness of the theoretical formulas using experimental data. Finally, a finite element analysis is employed to explore the impact of bolt physical parameters on the bolt preload, further validating the accuracy of the theoretical formulas through finite element modeling. The aim is to provide insights for the detection of related bolt forces.

2. Theoretical Analysis

In order to better understand the bolt-pulling process and the force mechanics acting on the bolt during pulling detection, a simplified single bolt-pulling model is used for derivation and analysis. The simplified model is shown in Figure 1.

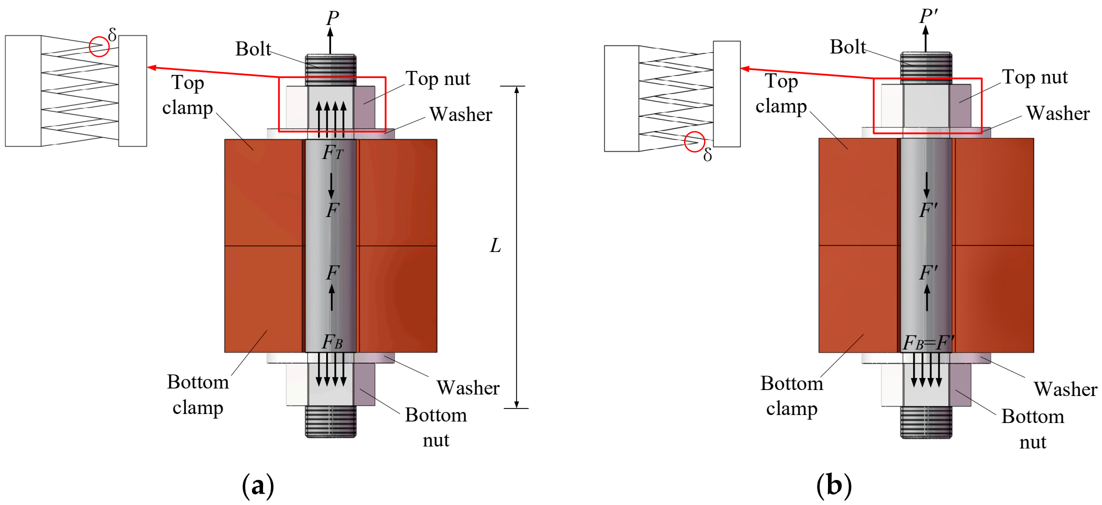

Figure 1. Simplified model of a single bolt (**a**) before the nut is loosened and (**b**) after the nut is loosened.

The bolt can be divided into two regions: the clamping section and the non-stress section. δ is the gap caused by thread fit. Assuming the preload in the clamping section of the bolt varies continuously during the tensioning process, the nuts and washers are considered to be rigid, and the length and deformation of the nuts and washers are neglected.

When a tensile force is applied to the end of the non-stress section, the gap δ between the threads gradually decreases, causing the bolt clamping section to elongate, thereby increasing the preload in the clamping section gradually. When the elongation of the clamping section equals δ, the nut becomes loose. At this point, if the tensile force continues to be applied, both the clamping section and the non-stress section are subjected to force. Therefore, the increase in preload during pull-out detection should be attributed to the gap between the threads, with the increment being the force required for the bolt to elongate by δ, expressed as follows:

$$F_i = \frac{\delta EA}{L} \tag{1}$$

where E is Young's modulus taken as 210 GPa, A is the bolt area, δ is the gap between the threads, L is the clamping section bolt length, and F_i is the increment of preload.

From the Equation (2), it can be observed that when the bolt clamping section length remains constant, the increment of preload increases with the increase in the bolt area; conversely, when the bolt area remains constant, the increment of preload decreases with the increase in the clamping section length.

To investigate the force relationship of the bolt during the pulling process, a similar analysis can be conducted as shown in Figure 1. In Figure 1, F represents the continuously changing axial force in the bolt, P is the tensile force, F_B is the preload exerted on the bolt by the bottom (non-tensioned end) nut according to the principle of action and reaction (which is equivalent to the support force experienced by the bottom nut), and F_T is the preload exerted on the bolt by the top (tensioned end) nut, which is equal to the supporting force experienced by the top nut.

Before the top nut is loosened, as tensile force P increases, the force F_T acting on the top nut decreases, while the force F_B acting on the bottom nut increases. Simultaneously, the elongation of the bolt leads to an increase in the preload F in the clamping section. Taking the vertical upward as the positive direction, according to the equilibrium equation, the following formula can be obtained:

$$P = F - F_T \tag{2}$$

$$F = F_B \tag{3}$$

Plugging Equation (3) in Equation (2),

$$P = F_B - F_T \tag{4}$$

During the tension process in the pull-out method, the tension force continually increases; as the tension force continuously increases from P_1 to P_2, it is assumed that:

$$P_2 - P_1 = (F_{B2} - F_{T2}) - (F_{B1} - F_{T1}) \tag{5}$$

$$\Delta P = \Delta F_B - \Delta F_T \tag{6}$$

After the top nut is loosened, there is no force in the top nut anymore. At this moment, the magnitude of the preload $F\prime$ is equal to the tensile force $P\prime$ that has been applied:

$$P\prime = F_B = F' \tag{7}$$

$$F_T = 0 \tag{8}$$

According to the analysis results of the simplified model, it can be found that during the process of pull-out detection, before the tensioned-end nut is loosened, the force in the bolt clamping section undergoes variation due to the gap of threads, resulting in an increment in the measured preload. After the tensioned-end nut is loosened from the washer, the bolt preload is equal to the tensile force and increases synchronously with it. Furthermore, throughout the entire process of the pull-out method, there exists a force relationship whereby the change in tension force is equal to the change value of the bottom nut force minus the change value of the top nut force.

3. Full-Scale Test

3.1. Full-Scale Test Device

The experimental device consisted of a bolt, a nut, a washer, a steel plate, a steel sleeve, a jack, pressure sensor 1, and pressure sensor 2; the whole experimental setup is shown in Figure 2.

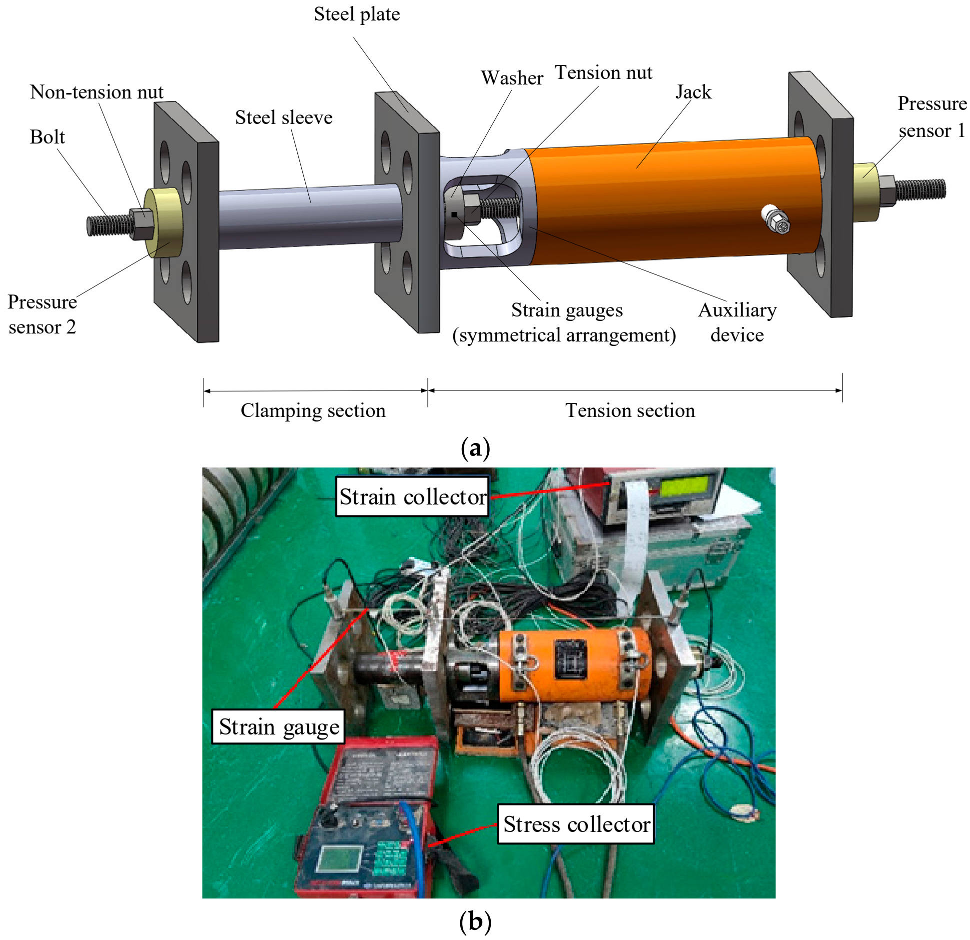

Figure 2. Full-scale test device. (**a**) Schematic diagram of experiment device components. (**b**) Device experiment diagram.

The bolt used had a diameter of 27 mm, a length of 1000 mm, and a tensile strength of 980 MPa. The washer had an outer diameter of 80 mm, an inner diameter of 40 mm, and a height of 27 mm. The steel sleeve, a device simulating a cable clamp, had an outer diameter of 80 mm, a height of 200 mm, and a thickness of 30 mm. The steel sleeve ensures that the preload is maintained. The auxiliary device acts as a holding force device and makes it easier to anchor the nut and measure the washer strain with the help of three holes. The steel plate had a thickness of 30 mm to withstand compressive forces.

A hydraulic jack was used as a tension device to induce displacement in the tension section. The tension force is applied to the bolt through the auxiliary device, which affects the bolt tension. Pressure sensor 1 was a JMZX-3110HAT under the jack with an accuracy of 0.1 kN, which was used to monitor jack force on the right side. Pressure sensor 2 was an FDBG-27-200 strain gauge pressure sensor under the non-tension nut with an accuracy of 0.01 kN, which was used to monitor preload changes on the clamping section's left side. Strain gauges 1 and 2 were symmetrically attached to both sides of the washer on the hydraulic jack's holding device to assist in evaluating the status of the nut.

As the tension nut loosens and separates from the washer, the trend of the strain changes, indicating that the strain image has a turning point and can be used to judge whether the nut is loosened. A hydraulic jack was used to apply an initial preload to the bolt, simulating the tension force of the bolt in a real bridge structure when using the pull-out method.

The experimental steps were as follows:

(1) Use the hydraulic jack to apply a certain amount of tension to the bolt.

(2) When the tension force on the bolt reaches the object value, tighten the nut through the clearance in the auxiliary device. Record the actual preload on the bolt measured by the vibrating wire pressure sensor (representing the actual preload) and the strain values on the washer.
(3) Use the hydraulic jack to gradually apply tensile loads step by step, and measure the values of the vibrating wire pressure sensor and the strain on the washer at each load level.
(4) Continuously monitor the strain data on the washer in real time. When a turning point is detected in the strain values, indicating that the nut is loosened, stop the tension operation and record each sensor reading.

3.2. Full-Scale Test Result

The experiment was carried out according to the experiment device in Figure 2. The experimental data under various levels of tensile force using the pulling method are shown in Tables 1 and 2. Load case 1 and 2, respectively, set bolt preloads of 26 kN and 27 kN.

Table 1. Changes in strain and pressure in load case 1 (the effective preload of the bolt is 26 kN).

Tension / Test Data	0 kN	20 kN	30 kN	40 kN	50 kN	60 kN	70 kN	80 kN	90 kN	100 kN	110 kN	120 kN
Pressure sensor 1 (kN) ①	0	21.4	30.2	37.9	43.8	55.8	66.8	73.0	83.3	95.1	108.0	120.0
Pressure sensor 2 (kN) ②	25.77	29.92	32.89	36.80	40.36	48.64	57.94	62.98	72.07	85.11	94.43	105.37
Strain gauge 1 strain value $\varepsilon 1$ ($\mu\varepsilon$)	39	34	26	19	14	6	4	3	2	2	2	3
Strain gauge 2 strain value $\varepsilon 2$ ($\mu\varepsilon$)	30	13	5	4	4	3	1	0	1	1	0	2
Washer pressure calculation value ③	27.31	18.60	12.27	9.10	7.12	3.56	1.98	1.19	1.19	1.19	0.79	1.98

Table 2. Changes in strain and pressure in load case 2 (the effective preload of the bolt is 27 kN).

Tension / Test Data	0 kN	20 kN	30 kN	40 kN	50 kN	60 kN	70 kN	80 kN	90 kN	100 kN	110 kN	120 kN
Pressure sensor 1 (kN) ①	0	24.0	31.0	38.4	43.9	51.5	58.2	71.5	83.6	95.3	106.9	117.0
Pressure sensor 2 (kN) ②	27.16	31.02	34.26	37.67	41.16	45.98	51.76	62.47	73.20	83.74	94.54	103.83
Strain gauge 1 strain value $\varepsilon 1$ ($\mu\varepsilon$)	41	34	29	22	17	10	8	5	5	5	4	6
Strain gauge 2 strain value $\varepsilon 2$ ($\mu\varepsilon$)	29	13	9	5	5	5	5	3	3	3	2	2
Washer pressure calculation value ③	27.71	18.60	15.04	10.69	8.71	5.94	5.15	3.17	3.17	3.17	2.37	3.17

It can be seen from Tables 1 and 2, after the nut is anchored and the jack is removed, that the washer pressure at the tension end can be calculated by the following:

$$F = \sigma A = EA(\varepsilon_1 + \varepsilon_2)/2 \tag{9}$$

where

E is Young's modulus taken as 210 GPa,
ε_1 is the strain value of the washer strain gauge 1,
ε_2 is the strain value of the washer strain gauge 2,
A is the washer area 3769.8 mm^2.

F is actually the pressure of the tension end nut. F is the same value as the pressure sensor 2 at the other end of the bolt and equal to the preload; this corresponds to the actual situation, therefore it can be considered that the data of the two groups of experiments are accurate and can be analyzed in the next step. Figures 3 and 4 show the change trend of the strain value data of the washers at the tension end of load case 1 and 2. The total change in force during the bolt tension process is shown in Figures 5 and 6.

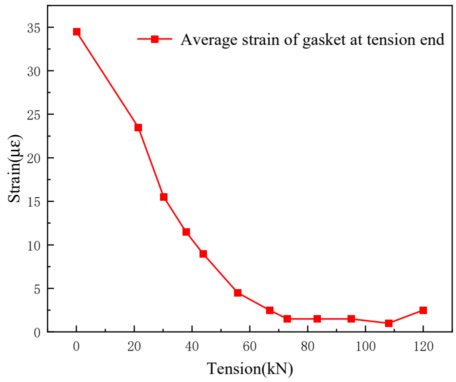

Figure 3. Washer strain data of load case 1.

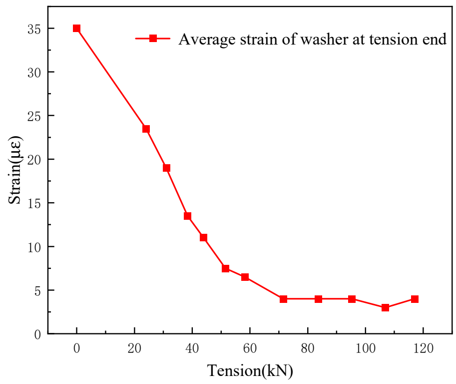

Figure 4. Washer strain data of load case 2.

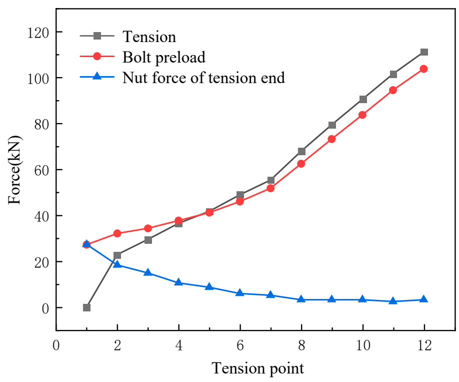

Figure 5. The force data of the bolt in load case 1.

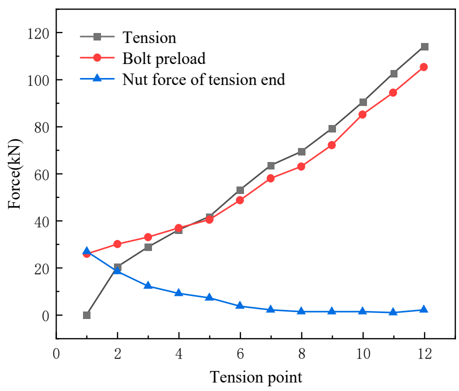

Figure 6. The force data of the bolt in load case 2.

After the tension nut is anchored, the pressure value measured by pressure sensor 2 is defined as the magnitude of the bolt preload. The calculated value of the washer pressure is the force of the tensioned-end nut. As shown in Figures 3 and 4, the strain values on the washers gradually decrease as the tensile force is gradually increased. When the strain values on the washers are close to zero, it is possible to loosen the nut manually, indicating that the nut has separated from the washer at that time.

Analysis of Figures 5 and 6 shows that the desired preload of the bolt gradually increases with the growth of the tensile force. In the initial stage, the growth rate of the preload is lower than the tensile force. However, when the bolt preload is equal to the tensile force, the bolt preload increases synchronously with the tensile force. It can be considered that when the preload is equal to the tensile force, the nut begins to loosen. At this point, the tension force is not the initial desired preload of the bolt, but rather it is greater than the initial desired preload. This means that the preload values obtained by the pull-out method are higher than the actual values, which is consistent between the experimental phenomena and theoretical analysis.

To analyze the relationship between the change value of the non-tensioned end force (preload), the change value of the tensioned end force, and the change value of the tension force before the nut is loosened, the change values of these three forces in the FE model were extracted, and are summarized in Table 3.

Table 3. Tensile force and the change value of nut force at both ends (experiment).

Load Case	Pressure Change Value of Non-Tensioned End Nut (N) ①	Pressure Change Value of Tensioned-End Nut (N) ②	The Difference between the Nut Force Change at Both Ends (N) ③ = ① − ②	Tension Change Value (N) ④	Difference and Tension Deviation (%) (③ − ④)/④
Load case 1	2.97	−6.33	9.30	8.8	5.68
	3.91	−3.17	7.08	7.70	−8.05
	3.56	−1.98	5.54	5.90	−6.10
	8.28	−3.56	11.84	12.00	−1.33
	9.3	−1.58	10.88	11.00	−1.09
Load case 2	3.24	−3.56	6.80	7.00	−2.86
	3.41	−4.35	7.76	7.40	4.86
	3.49	−1.98	5.47	5.50	−0.55
	4.82	−2.77	7.59	7.60	−0.13
	5.78	−0.79	6.57	6.70	−1.94

From Table 3, it can be seen that the difference between the bolt preload (change in force on the non-tensioned end nut) and the force change on the tensioned end nut is exactly equal to the change in tensile force (within 10% error). This result is consistent with Equation (6) derived from theoretical analysis.

4. Finite Element Analysis

4.1. Finite Element Model and Verification

To facilitate the verification of the FE model, the experimental study on load case 1 was simulated. In the FE model, the geometry and material parameters were taken according to the test specimen: a 27 mm diameter bolt with a length of 1000 mm; the height of the top and bottom nuts is 50 mm, and the inner diameter is 27 mm. A support body with dimensions of 350 mm × 350 mm × 800 mm was modeled using ANSYS WORKBENCH (2021). The primary focus of this study is the variation of forces on the bolt during a tensile loading process; therefore, the detailed structure of the threads is neglected. The bolt, nuts, and support body were modeled using SOLID45. They are all made of 40Cr alloy steel, and the material parameters can be found in Table 4. A bilinear constitutive model is applied to the material and its stress–strain relationship can be expressed as follows:

$$\sigma = \begin{cases} E\varepsilon & \varepsilon \leq \frac{\sigma_y}{E} \\ \sigma_y + H(\varepsilon - \frac{\sigma_y}{E}) & \varepsilon > \frac{\sigma_y}{E} \end{cases} \tag{10}$$

where, σ is stress, E is elastic modulus, ε is strain, σ_y is yield stress, and H is the strain hardening rate.

Table 4. Material parameters of alloy steel.

Material	Density (kg/m^3)	Elastic Modulus (GPa)	Poisson's Ratio	Yield Stress (MPa)	H (GPa)
40Cr	7800	210	0.3	835	21

The nominal element size is taken as 5 mm. The boundary conditions of the finite element model are as follows: surface-to-surface contact is used for each contact surface in the model; a bonded contact is defined between the bolt and the nut, while a friction coefficient of 0.3 is defined between the top and bottom surfaces of the support body and the nut; the bottom surface of the support body is fixed to eliminate rigid displacements in the calculations. The FE model is shown in Figure 7.

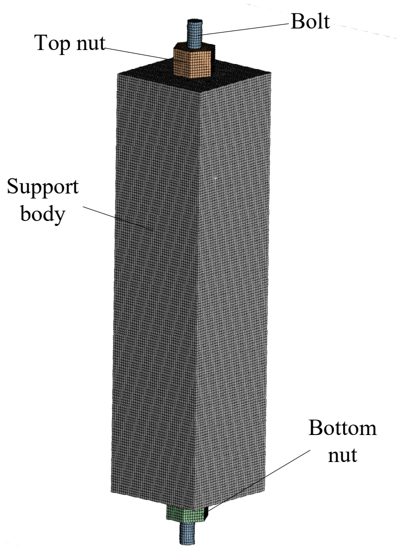

Figure 7. Finite element model of pull-out method.

A 12-step FE analysis was carried out based on the above-mentioned FE model. In the first step (i.e., the static procedure), a 26 kN preload is applied to the bolt using the BOLT PRELOAD option provided by ANSYS WORKBENCH. In the remaining eleven steps, a vertical top tension force is applied to the top of the bolt. The tension force increases from 0 kN to 120 kN as the analytical steps run with the increment of load case 1.

The FE results were compared with the experimental data in terms of the preload variation curve (see Figure 8). It was found that the bolt behavior is well reproduced by the developed FE model. The changes in the preload of the bolt are also in good agreement with the experimental observation.

4.2. Finite Element Result

Utilizing the FE model established through load case 1, the process of the pull-out method was studied. The Mises stress diagrams for after the bolt preload is applied and the pulling detection stage are shown in Figures 9 and 10. These figures represent the stress distribution in the bolt during the anchoring completion and pulling stages.

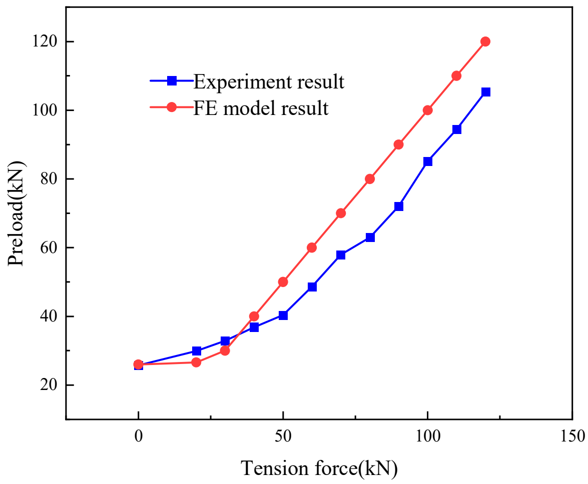

Figure 8. The curve of the FE model compared with load case 1.

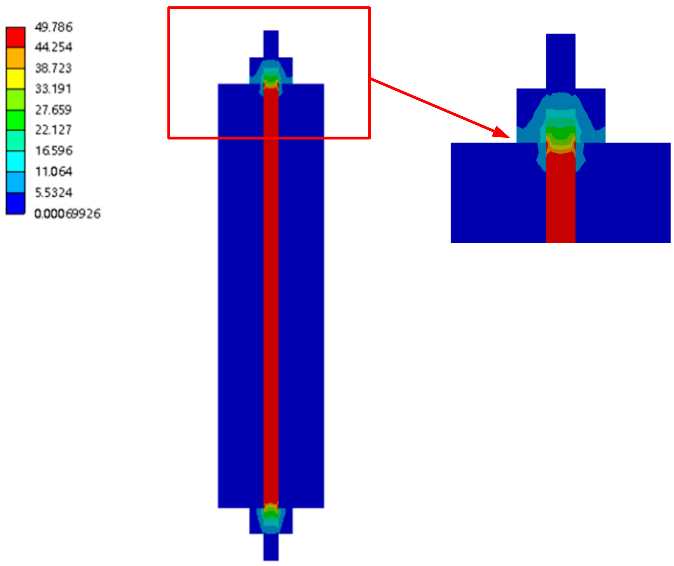

Figure 9. Stress diagram of the bolt after clamping.

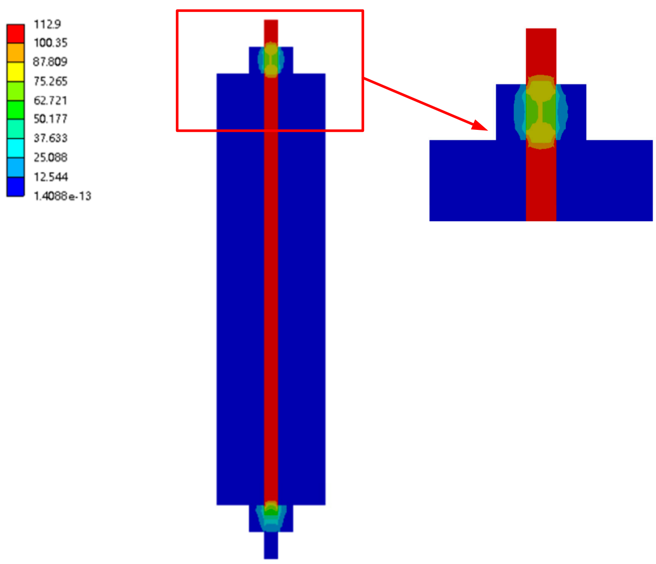

Figure 10. Stress diagram of the bolt during pulling process.

As depicted in Figures 9 and 10, it can be seen that the equivalent stress reaches its maximum at the junction of the bolt and nut, and gradually decreases in the surrounding regions, indicating a significant stress concentration at the interface. During the pulling period, the bolt preload increases, accompanied by a decrease in the stress on the top nut. To further analyze the stress variations in the nut and bolt, the tensile force and the force of the nuts at the top and bottom ends were obtained, as shown in Figure 11.

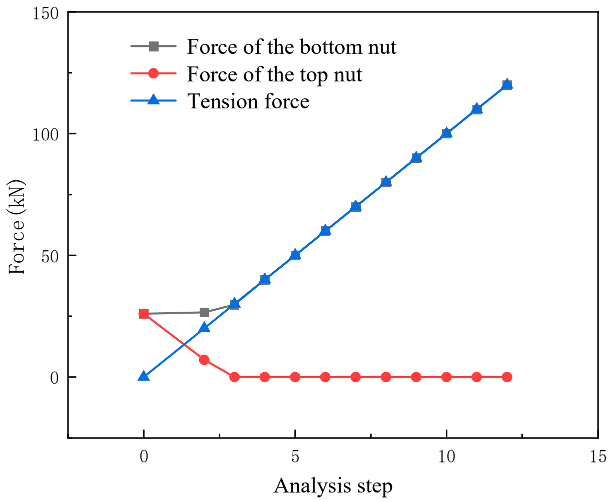

Figure 11. Tension force and force values at the top and bottom nuts.

As depicted in Figure 11, it can be observed that during the pulling process, the force exerted by the bottom nut gradually increases while the force exerted by the top nut decreases. When the force exerted by the top nut decreases to zero, the forces exerted by the bottom nut and the tension force increase synchronously. This is consistent with the experimental results. To verify the force relationship of each component of the bolt obtained in the experiment and theoretical analysis, the change in tensile force during the selected pulling process and the pressure variations in the contact pairs between the top and bottom nuts and support body were obtained. These values are shown in Table 5.

Table 5. Tension force and nut pressure change value (finite element).

Bottom Nut Pressure Change Value (N) ①	Top Nut Pressure Change Value (N) ②	The Difference between the Nut Force Change at Both Ends (N) ③ = ① − ②	Tension Change Value (N) ④	Difference and Tension Deviation (%) |③ − ④|/④
115	−3786	3901	4000	2.4
115	−3785	3900	4000	2.5
172	−5678	5850	6000	2.5
173	−5678	5851	6000	2.5
57	−1893	1950	2000	2.5
60	−1889	1949	2000	2.6

As depicted in Table 5, the change in tensile force is equal to the difference in pressure variation between the bottom nut and the top nut during the tensile process, which is the same as for the experimental results and theoretical analysis.

4.3. Parametric Study

During the pull-out detection process, there is an increment in the preload. The theoretical form of the increment is represented by Equation (1). It can be inferred from Equation (1) that the factors influencing the increment include the length of the clamping section and the bolt area. To investigate the impact of the bolt clamping section length and the bolt area on the bolt preload, three different working conditions were designed for each influencing factor.

4.3.1. Clamping Section Length

To investigate the effect of the clamping section length of the bolt on the preload increment, three different operating conditions were designed, and FE models were established for each condition. Every model consists of bolt, support body, and nuts. The bolt diameter is 27 mm and the length is 800 mm. The lengths of the support body are 600 mm, 500 mm, and 400 mm, respectively. The nut height is 50 mm, with an inner diameter of 27 mm. Therefore, the clamping section lengths for the three operating conditions are 600 mm, 500 mm, and 400 mm, respectively. The bolt, nuts, and support body were modeled using SOLID45. They are all made of 40Cr alloy steel, and the material parameters can be found in Table 4.

In order to reduce the computation time of the model without compromising its accuracy, the element size of the support body is set to 10 mm, while the element size of other components is set to 5 mm. The boundary conditions of the model are consistent with the previous paper. A 16-step FE analysis was carried out based on the above-mentioned FE model. In the first step (i.e., the static procedure), a 50 kN preload is applied to the bolt using the BOLT PRELOAD option provided by ANSYS WORKBENCH. To study the correlation between the preload and tension force, a vertical top force is applied in the following analytical steps on the top end of the bolt: the tension force increases from 10 kN to 150 kN as the analytical steps run; the nut is considered to have loosened when the pressure at the top nut (tensioned end) reaches zero. The FE models corresponding to the three operating conditions are depicted in Figure 12.

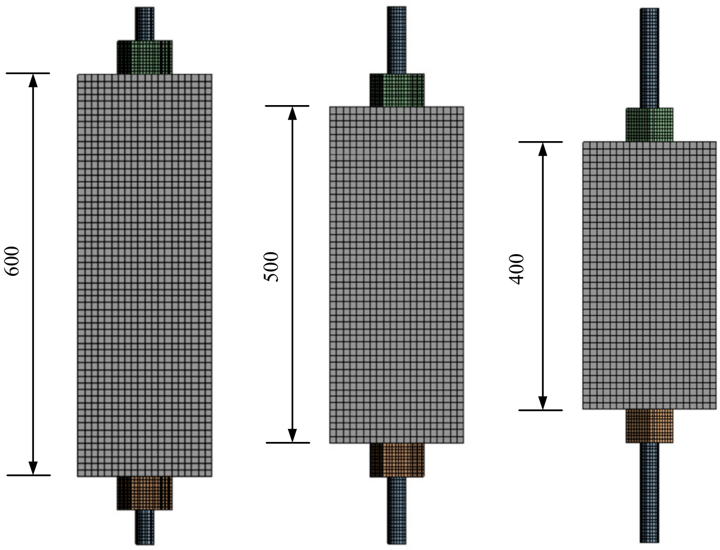

Figure 12. The FE models of different clamping section lengths (Unit: mm).

The preload corresponding to the FE models under three different operating conditions were extracted to study the influence of the clamping section length on the incremental preload during the tensioning process. The preload for different clamping section lengths are presented in Figure 13.

As depicted in Figure 13, it can be observed that under the same bolt area, a shorter clamping section length corresponds to a greater increase in preload, which is consistent with the theoretical results of Equation (1). However, when viewed as a whole, the three data lines almost overlap with little variation. This indicates that while the clamping section length does have an impact on the increase in preload, the effect is relatively minor.

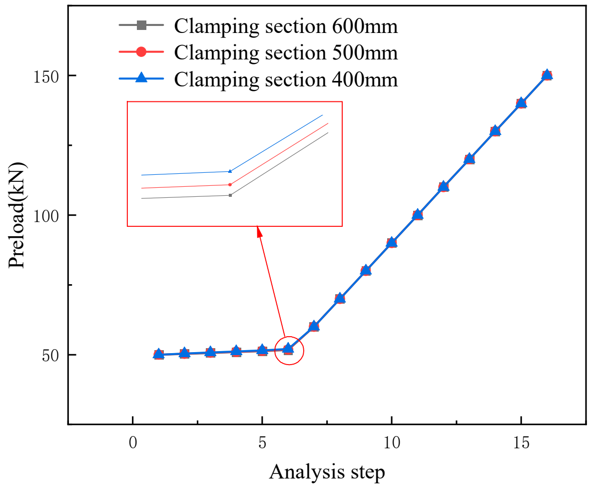

Figure 13. Preload for the different clamping section lengths.

4.3.2. Bolt Area

To investigate the effect of the bolt area on the preload increment, three different operating conditions were designed and FE models were established for each condition. Every model consists of a bolt, support body, and nuts. The bolt length is 800 mm, and the bolt diameter is, respectively, 25 mm, 30 mm, and 35 mm. The dimensions of the support body are 350 × 350 × 600 mm. The nut height is 50 mm, with an inner diameter of 27 mm. The bolt, nuts, and support body were modeled by using SOLID45. They are all made of 40Cr alloy steel, and the material parameters can be found in Table 4.

The element size of the support body is set to 10 mm, while the element size of other components is set to 5 mm. The boundary conditions of the model are consistent with the previous paper. A 16-step FE analysis was carried out based on the above-mentioned FE model. In the first step (i.e., the static procedure), a 50 kN preload was applied to the bolt using the BOLT PRELOAD option provided by ANSYS WORKBENCH. To study the correlation between the preload and tension force, a vertical top force is applied in the following analytical steps on the top end of the bolt: the tension force increases from 10 kN to 150 kN as the analytical steps run; the nut is considered to have loosened when the pressure at the top nut (tensioned end) reaches zero. The FE models corresponding to the three operating conditions are depicted in Figure 14.

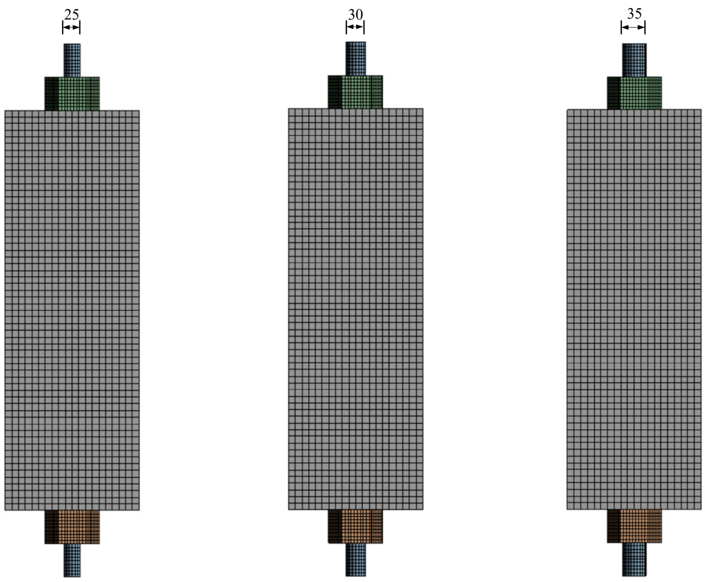

Figure 14. The FE models of different bolt areas (Unit: mm).

The preload corresponding to the FE models under three different operating conditions were extracted, to study the influence of the bolt area on the incremental preload during the tensioning process. The preload for different bolt areas are presented in Figure 15.

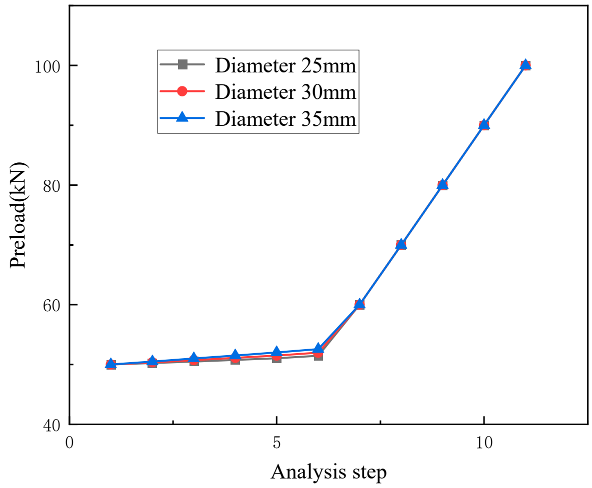

Figure 15. Preload for different bolt areas.

As depicted in Figure 15, with the same clamping section length, the increment of preload increases with the bolt area, which is consistent with the theoretical results of Equation (1). Furthermore, the influence of bolt area on the increase in preload is greater than clamping section length.

5. Discussion

In both of our experiments, the washer strain values did not completely reach zero and exhibited fluctuations. This may be attributed to the residual elastic strain generated by the 40Cr material, which maintains a certain level of elastic deformation even after the stress is removed. The deviation between the values of the force change at both ends of the nut and the tensile force during the experiment is larger than the results of the finite element simulation. This difference may be due to variations in the boundary conditions between the bolt and various components in the experimental set compared to the finite element model. In addition, the horizontal experimental set introduces gaps in the installation of pressure sensors and various components, which may cause inelastic deformations such as compression between components during certain stages of tensile force variation.

Preload bolts are typically divided into a non-stress section and a clamping section. Some detection methods assume that the force in the clamping section remains constant [30,34]. However, our experiments and FE model results share a common phenomenon. With the gradual increase in the tension force, the pressure on the nut at the top end (tensioned end) decreases, while the pressure on the nut at the bottom end (non-tensioned end) slowly increases. This indicates that the preload in the clamping section is not constant, but increases gradually during the pulling period. This study shows that in the pull-out method, the preload acting on the bolt gradually increases with the tension force. When the nut starts to loosen, the tension force does not represent the initial preload of the bolt but is larger than the actual preload. The increase in preload during the pull-out detection should be attributed to the gap between the threads. The change in tension force is equal to the difference in force changes between the non-tensioned end nut (bolt preload) and the tensioned end nut. This further explains that the error in the pull-out method of detection may be due to the variation of the preload during the detection process. This paper also explores the impact of clamping section length and bolt area on this detection error. This paper indicates that the detection accuracy can be improved by aiming to reduce such errors or by further utilizing the relationship between the tension force and the preload for detection purposes.

6. Conclusions

This paper combines theoretical analysis, full-scale test, and finite element analysis to investigate the force principles involved in the pull-out detection process and explore the influence of a bolt's physical parameters on the bolt force. The following conclusions were obtained:

(1) During the pull-out method detection process, the bolt preload increases. Therefore, the preload detected by the pull-out method is not the initial preload of the bolt, but rather it exceeds the initial preload.

(2) The reason for the increase in preload is due to the gap δ between the threads, and under the same conditions, the increment of preload is a constant value. The theoretical value of this constant is $F_i = \frac{\delta EA}{L}$. One can consider increasing the bolt preload design value by F_i.

(3) There is a close relationship between the tension force and the preload, where the change in the tension force is equal to the difference between the changes in the pressure of the non-tensioned end of the nut (bolt preload) and the tensioned end of the nut.

(4) Under the same bolt area, a shorter clamping section length corresponds to a greater increase in preload. With the same clamping section length, the increment of preload increases with the bolt area. The influence of bolt area on the increase in preload is greater than that of clamping section length.

Author Contributions: Conceptualization, F.M.; methodology, Y.Z. (Yongjun Zhou); software, Y.J.; validation, F.M., Y.Z. (Yongjun Zhou) and Y.J.; formal analysis, F.M.; investigation, F.M.; resources, Y.Z. (Yu Zhao) and Z.J.M.; data curation, F.M.; writing—original draft preparation, F.M. and Y.Z. (Yongjun Zhou); writing—review and editing, F.M., Y.Z. (Yongjun Zhou) and Y.J.; visualization, F.M. and Y.J.; supervision, Y.Z. (Yu Zhao) and Z.J.M.; project administration, Y.Z. (Yu Zhao); funding acquisition, Y.Z. (Yongjun Zhou) and G.Z. All authors have read and agreed to the published version of the manuscript.

Funding: This research was funded by National Key R&D Plan (2021YFB1600300) and Guangxi Department of Science and Technology Key R&D Plan (AB23026125).

Data Availability Statement: The data presented in this study are available from the first and corresponding author upon request. The data are not publicly available due to the policy of the data provider.

Conflicts of Interest: Author Gui Zhu was employed by the company Guangxi Xingang Transportation Investment Co., Ltd. The remaining authors declare that the research was conducted in the absence of any commercial or financial relationships that could be construed as a potential conflict of interest.

References

1. Zhang, P.F. Reason analysis and preventive maintenance countermeasures for the decrease of pre-tightening force of cable clamp bolt of suspension bridge. *Highway* **2019**, *64*, 101–105.
2. Li, H.; Liu, Y.; Li, C.; Hu, H.; Sun, Q. Force analysis of self-anchored suspension bridges after cable clamp slippage. *Symmetry* **2021**, *13*, 1514. [CrossRef]
3. Wang, Q.A.; Zhang, C.; Ma, Z.G.; Ni, Y.Q. Modelling and forecasting of SHM strain measurement for a large-scale suspension bridge during typhoon events using variational heteroscedastic Gaussian process. *Eng. Struct.* **2022**, *251*, 113554. [CrossRef]
4. Petersen, Ø.W.; Øiseth, O.; Lourens, E.M. Estimation of the dynamic response of a slender suspension bridge using measured acceleration data. *Procedia Eng.* **2017**, *199*, 3047–3052. [CrossRef]
5. Nicoletti, V.; Quarchioni, S.; Tentella, L.; Martini, R.; Gara, F. Experimental tests and numerical analyses for the dynamic characterization of a steel and wooden cable-stayed footbridge. *Infrastructures* **2023**, *8*, 100. [CrossRef]
6. Nikravesh, S.M.Y.; Goudarzi, M. A review paper on looseness detection methods in bolted structures. *Lat. Am. J. Solids Struct.* **2017**, *14*, 2153–2176. [CrossRef]
7. Nassar, S.A.; Sun, T.; Zou, Q.B. *The Effect of Coating and Tightening Speed on the Torque-Tension Relationship in Threaded Fasteners*; SAE International: Warrendale, PA, USA, 2006.
8. Zou, Q.; Sun, T.S.; Nassar, S.A.; Barber, G.C.; Gumul, A.K. Effect of lubrication on friction and torque-tension relationship in threaded fasteners. *Int. Jt. Tribol. Conf.* **2007**, *50*, 127–136. [CrossRef]

9. Wang, Z.; Zhang, Z.; Cui, C. Measurement and control method for miniature fastener tension in precision instrument. *Procedia CIRP* **2018**, *76*, 110–114. [CrossRef]
10. Nazarko, P.; Ziemianski, L. Force identification in bolts of flange connections for structural health monitoring and failure prevention. *Procedia Struct. Integr.* **2017**, *5*, 460–467. [CrossRef]
11. Pan, Q.; Pan, R.; Shao, C.; Chang, M.; Xu, X. Research review of principles and methods for ultrasonic measurement of axial stress in bolts. *Chin. J. Mech. Eng.* **2020**, *33*, 1–16. [CrossRef]
12. Jhang, K.Y.; Quan, H.H.; Ha, J.; Kim, N.Y. Estimation of clamping force in high-tension bolts through ultrasonic velocity measurement. *Ultrasonics* **2006**, *44*, 1339–1342. [CrossRef] [PubMed]
13. Pan, Q.; Pan, R.; Chang, M.; Shao, C.; Liu, X.; Xu, X. Reliability evaluation of bolt fastening force based on ultrasonic measurement method. In Proceedings of the 2019 IEEE International Conference on Mechatronics and Automation (ICMA), Tianjin, China, 4–7 August 2019; pp. 2212–2217.
14. Moradi Kelardeh, S.; Hosseini, S.V.; Heidari, M.; Parvaz, H. An investigation of the effect of bolt tightening stress on ultrasonic velocity in cylinder head and main bearing cap bolts of diesel engine. *J. Braz. Soc. Mech. Sci. Eng.* **2021**, *43*, 375. [CrossRef]
15. Kim, N.; Hong, M. Measurement of axial stress using mode-converted ultrasound. *NDT&E Int.* **2009**, *42*, 164–169. [CrossRef]
16. Chen, P.; He, X.; Song, W. Parameter Recognition of Mode-Converted Wave in Single-Source Ultrasound Using Gabor Transform for Bolt Axial Stress Evaluation. *J. Sens.* **2020**, *2020*, 8883845. [CrossRef]
17. Pan, Q.; Pan, R.; Chang, M.; Xu, X. A shape factor based ultrasonic measurement method for determination of bolt preload. *NDT E Int.* **2020**, *111*, 102210. [CrossRef]
18. Sun, Q.; Yuan, B.; Mu, X.; Sun, W. Bolt preload measurement based on the acoustoelastic effect using smart piezoelectric bolt. *Smart Mater. Struct.* **2019**, *28*, 055005. [CrossRef]
19. Cai, Y.H.; Tao, S.; Zheng, X.D.; Yu, Q.; He, S.Y. Error analysis of measuring the axial force of the cable clamp screw using ultrasonic longitudinal wave method. *Highway* **2023**, *68*, 141–147.
20. Nazarko, P.; Ziemiański, L. Application of elastic waves and neural networks for the prediction of forces in bolts of flange connections subjected to static tension tests. *Materials* **2020**, *13*, 3607. [CrossRef]
21. Herbst, F.; Chadda, R.; Hartmann, C.; Peters, J.; Riehl, D.; Gwosch, T.; Hofmann, K.; Matthiesen, S.; Kupnik, M. Multi-Axis Force Sensor for Sensor-Integrating Bolts. In Proceedings of the 2022 IEEE Sensors, Dallas, TX, USA, 30 October 2022–2 November 2022.
22. Tu, Y.; Huang, Y.K.; Tu, S.T. Real-time monitoring of bolt clamping force at high temperatures using metal-packaged regenerated fiber Bragg grating sensors. *Int. J. Press. Vessel. Pip.* **2019**, *172*, 119–126. [CrossRef]
23. Wang, T.; Tan, B.; Lu, G.; Liu, B.; Yang, D. Bolt pretightening force measurement based on strain distribution of bolt head surface. *J. Aerosp. Eng.* **2020**, *33*, 04020034. [CrossRef]
24. Liu, S.; Sun, Z.; Ren, G.; Liao, C.; He, X.; Luo, K.; Li, R.; Jiang, W.; Zhan, H. Ultrasonic Measurement of Axial Preload in High-Frequency Nickel-Based Stoperalloy Smart Bolt. *Sensors* **2022**, *23*, 220. [CrossRef]
25. Jiménez-Peña, C.; Lavatelli, A.; Balcaen, R.; Zappa, E.; Debruyne, D. A Novel Contactless Bolt Preload Monitoring Method Using Digital Image Correlation. *J. Nondestruct. Eval.* **2021**, *40*, 54. [CrossRef]
26. Gotoh, Y.; Shigematsu, N. Slack Inspection Method of High-Tension Bolt Using Electromagnetic Field Without Influence of Lift-Off Between Bolt Head and Inspection Sensor. *IEEE Trans. Magn.* **2017**, *53*, 2500804. [CrossRef]
27. Mori, K.; Horibe, T.; Maejima, K. Evaluation of the axial force in an FeCo bolt using the inverse magnetostrictive effect. *Measurement* **2020**, *165*, 108131. [CrossRef]
28. Hasebe, K.; Wada, Y.; Nakamura, K. Non-contact bolt axial force measurement based on the deformation of bolt head using quartz crystal resonator and coils. *Jpn. J. Appl. Phys.* **2022**, *61*, SG1022. [CrossRef]
29. Hashimura, S.; Komatsu, K.; Inoue, C.; Nakao, T. A new tightening method of bolt/nut assembly to control the clamping force. *J. Adv. Mech. Des. Syst. Manuf.* **2008**, *2*, 896–902. [CrossRef]
30. Hashimura, S.; Komatsu, K. *Development of New Detecting Method of Clamping Force of Bolted Joint*; SAE Technical Paper; SAE International: Warrendale, PA, USA, 2007. [CrossRef]
31. Hashimura, S.; Komatsu, K.; Shinohara, N.; Nishioka, I.; Otsu, T. *Development of Detection Method for Clamped Part Stiffness in Bolted Joint*; SAE Technical Paper; SAE International: Warrendale, PA, USA, 2019. [CrossRef]
32. Hashimura, S.; Sakai, H.; Kubota, K.; Ohmi, N.; Otsu, T.; Komatsu, K. Influence of configuration error in bolted joints on detection error of clamp force detection method. *Int. J. Autom. Technol.* **2021**, *15*, 396–403. [CrossRef]
33. Hashimura, S.; Kubota, K.; Ohmi, N.; Komatsu, K. Robustness of detection method for clamp force against configuration error in bolt/nut assemblies. In *International Conference on Leading Edge Manufacturing/Materials and Processing*; American Society of Mechanical Engineers: New York, NY, USA, 2020; Volume 83624. [CrossRef]
34. Pan, Q.; Shao, C.; Xiao, D.; Pan, R.; Liu, X. Study of Ultrasonic Measurement Method for Bolt Fastening Force Based on Shape Factor. *Acta Armamentarii* **2019**, *40*, 880–888.